# Evaluating Saliency Models in Motion: DeepGaze IIE Outperforms Itti-Koch on Egocentric Video but Reveals a Performance Gap Beyond Static Viewing

## Experimental Design

**Core Question**
Can saliency models trained on static lab images predict human gaze in dynamic, real-world egocentric video?

**Experimental Setup**
7 participants walked two designated routes while wearing Tobii Pro Glasses 3, capturing natural gaze data and first-person video. No specific task instructions were given to ensure natural viewing behavior.

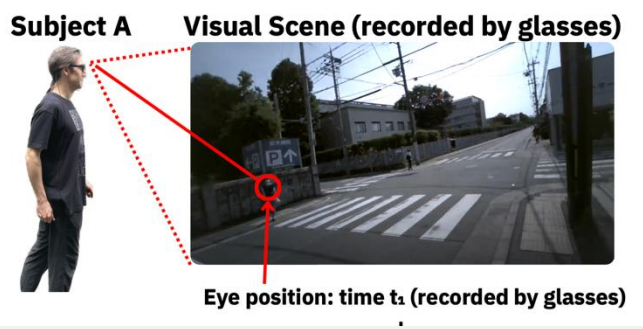


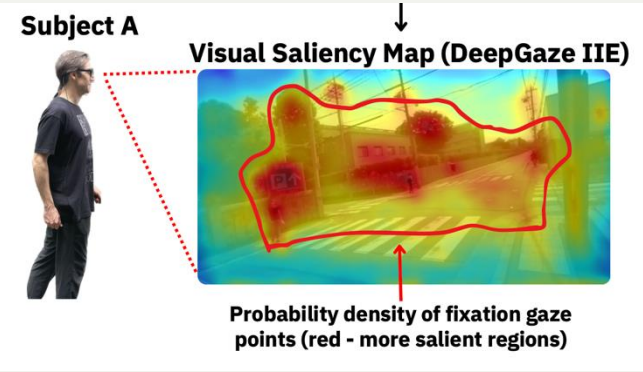


## Models being compared

**Classic Model**
**Itti-Koch (1998).**
A biologically-inspired model that simulates bottom-up attention by creating a saliency map from low-level visual features like color, intensity, and orientation.

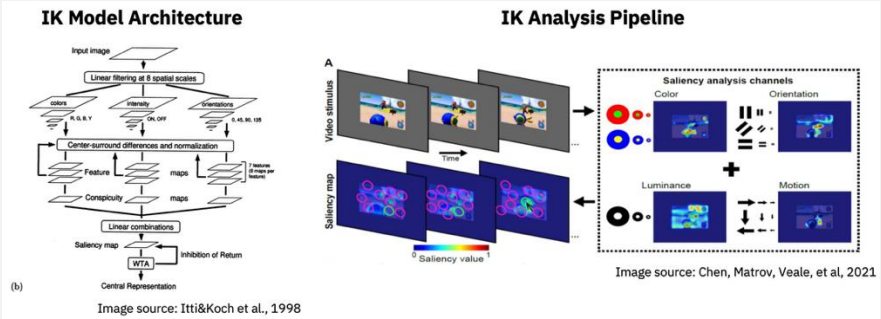


**Modern Model**
**DeepGaze IIE (2021).**
A deep learning model using a pre-trained Convolutional Neural Network (CNN) to extract high-level features. It was trained on large static image datasets (SALICON and MIT1003).

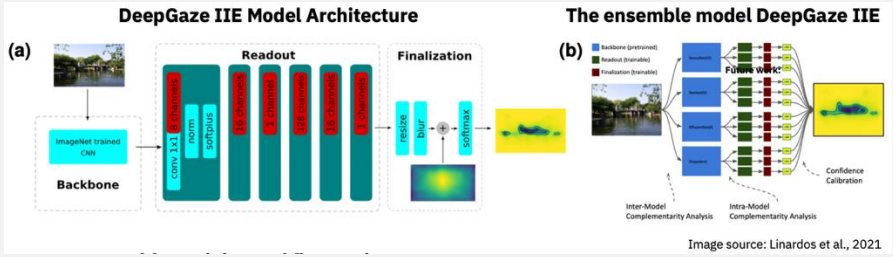


## Verdict & Key Insight

**Results**
DeepGaze IIE demonstrated superior performance across key metrics, indicating a better prediction of human gaze locations in this dynamic task.

**Key Insight**
Despite outperforming the classic model, DeepGaze IIE's overall performance was modest (AUROC of 0.574).
This suggests that models trained exclusively on static, lab-based images do not fully translate to the complexities of real-world, dynamic egocentric vision.

**Model Performance Comparison**

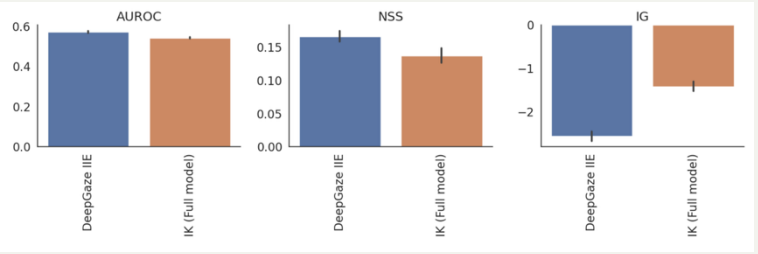


**Per-subject Model Performance Comparison**

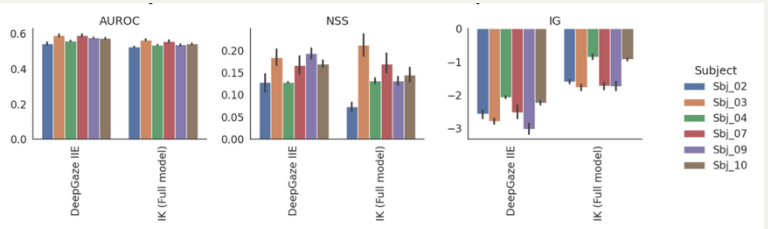

# A Recurrent Neural Network Model of Risk-Sensitive Choice

## 1. Hypothesis: Risk Preference Emerges from Asymmetric Reward Processing

**Core Question:** How do neural circuits give rise to the full spectrum of risk attitudes—from strong risk-aversion to active risk-seeking? In everyday decision-making, we frequently weigh safer, lower-return options (LL) against riskier alternatives that promise higher potential rewards (HH).

**Hypothesis:** Risk preference is driven by an imbalance in how the brain processes positive ("better-than-expected") and negative ("worse-than-expected") Reward Prediction Errors (RPEs).

**Conceptual Framework:**

- **Risk-Seeking ($n^+ > n^-$):** Overweighting positive RPEs inflates the value of volatile, high-return options.
- **Risk-Neutral ($n^+ = n^-$):** Treating negative and positive RPEs same.
- **Risk-Averse ($n^+ < n^-$):** Overweighting negative RPEs deflates the value of these high-return options.

**Learned EV Representation**

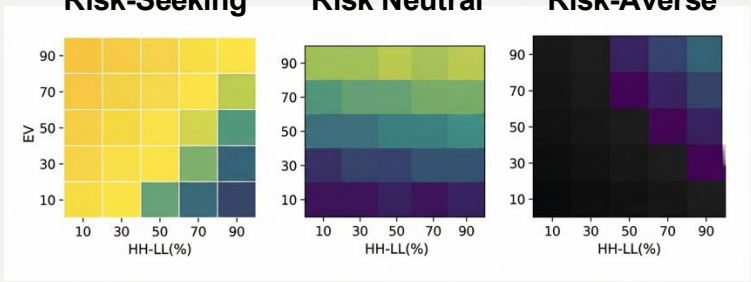


## 2. Model: A Biologically-Inspired Risk-Sensitive RNN

**Architecture:** A dual-component Recurrent Neural Network (RNN) was developed to test this hypothesis.

- **Policy Network (100 units):** Selects actions (Left, Right, Fixate).
- **Value Network (100 units):** Computes the predicted value **(V)** of potential choices.

**Network Architecture**

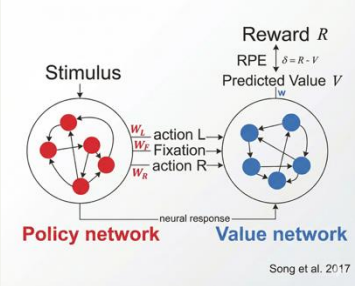


**Risk Sensitivity Representation**

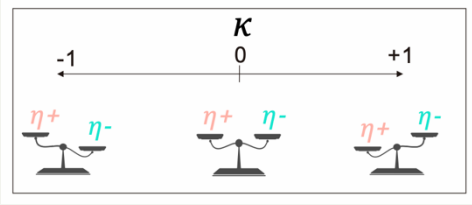


**Key Mechanism: The Risk-Sensitivity Parameter (κ)**

A single parameter κ is introduced to asymmetrically scale RPEs (δ) during learning, allowing for precise control over the model's risk attitude. The scaled RPE (δ′) is calculated as:

$$\delta' = \eta^+ \cdot \delta \text{ (if } \delta > 0)$$
$$\delta' = \eta^- \cdot \delta \text{ (if } \delta < 0)$$

Where:

- $\eta^+$ = 1 - κ (Scaling for positive RPEs)
- $\eta^-$ = 1 + κ (Scaling for negative RPEs)

**Training Protocol – 2-stage process:**

**Baseline Training:** A risk-neutral model (κ = 0) is first trained to full convergence on the decision task.

**Risk Fine-Tuning:** The converged model is then fine-tuned with specific non-zero κ values.

## 3. Results: Risk Parameter Causally Shapes Behavior and Neural Tuning

**Systematic Behavioral Shift:** Varying κ produces a full spectrum of choice behavior. A negative k induces a strong preference for high-risk options, while a positive k leads to consistent risk-averse choices.

**Choice Distribution**

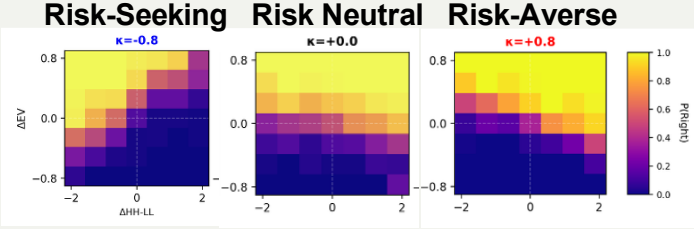


**Underlying Neural Reorganization:** This behavioral shift is directly mirrored by a reorganization of neural tuning in the Policy and Value networks.

**Value Network Neuron Distribution**

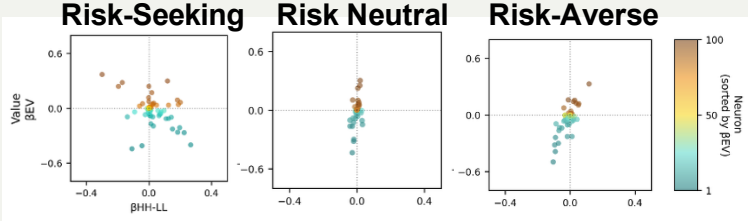


**Primary Finding:** Our model demonstrates a causal link between asymmetric RPE scaling, the reorganization of a neural population, and observabie risk-sensitive behavior.

# Classifying Schizophrenia with 88% AUROC Using Video-Based Eye-Tracking

## Distinct Gaze Patterns Differentiate Patients from Controls

21 schizophrenia patients and 13 healthy controls viewed videos of various scenes. Eye movements were recorded at 1000 Hz using an EyeLink 1000 Plus system.

### Overall Gaze Distribution

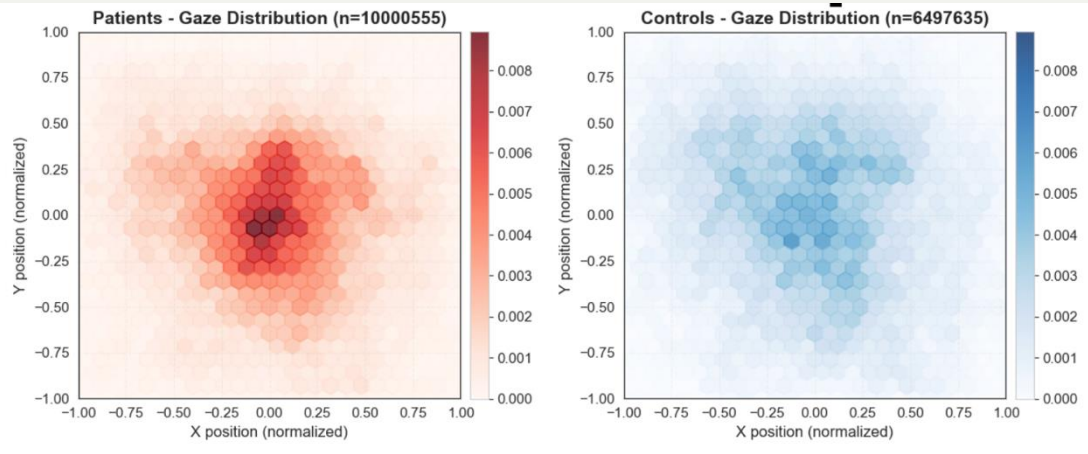


### Selected Features

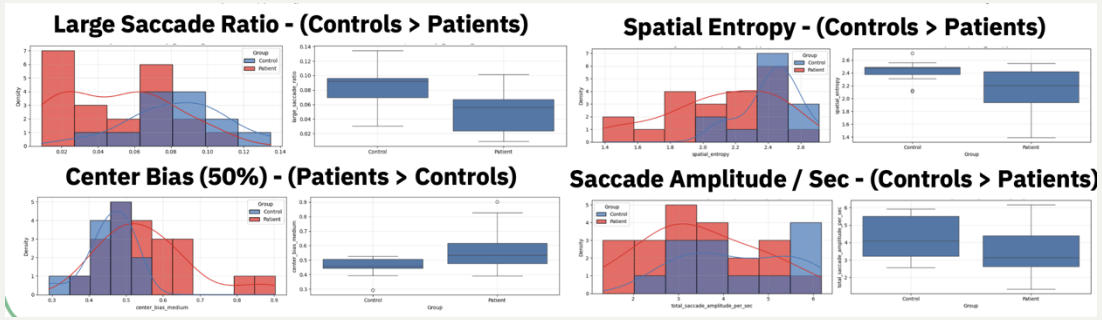


## A Logistic Regression Model Achieves High Diagnostic Accuracy

Following recursive feature elimination to identify the most discriminative signals, a Logistic Regression classifier was trained on just four key features:

- Large Saccade Ratio (>5°) (Higher in Controls)
- Spatial Entropy (Higher in Controls)
- Center Bias (50%) (Higher in Patients)
- Total Saccade Amplitude / Sec (Higher in Controls)

### ROC Curve

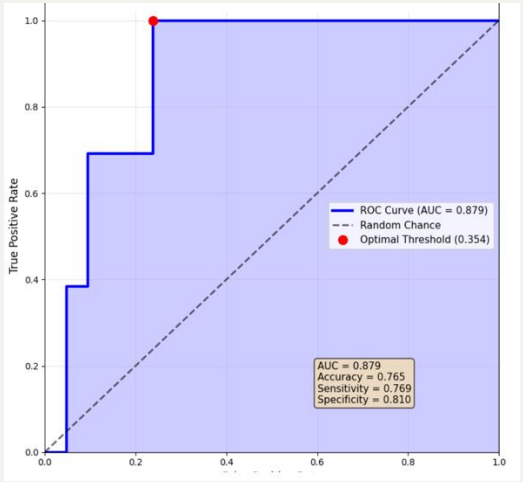


### Confusion Matrix

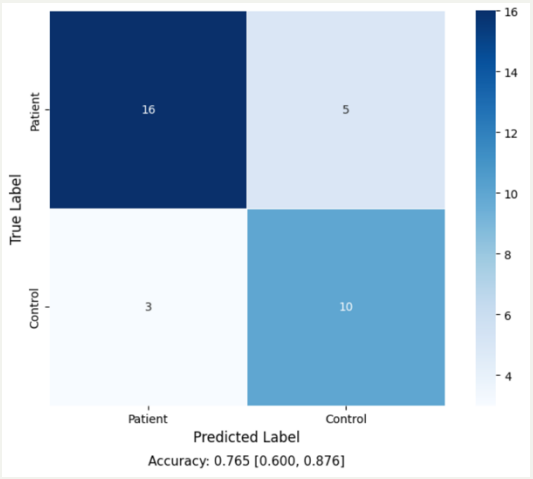


This work demonstrates that features extracted from eye movements during video-viewing can serve as a robust, objective, and non-invasive biomarker for schizophrenia, achieving accuracy comparable to previous image-based methods.

# DeepSpaceDB: a spatial transcriptomics atlas for interactive in-depth analysis of tissues and tissue microenvironments

**2,144** Total Samples (1361 Human, 783 Mouse)

**5.4 Million** Total Spots

Published in: *Nucleic Acids Research* (IF=17, first author)

### Search & Discover

Search a comprehensive, manually curated database by tissue, organism, condition, or publication to find relevant datasets.

### Interactive Exploration

Manually select any region of a tissue sample to perform on-the-fly differential gene expression analysis between your selections.

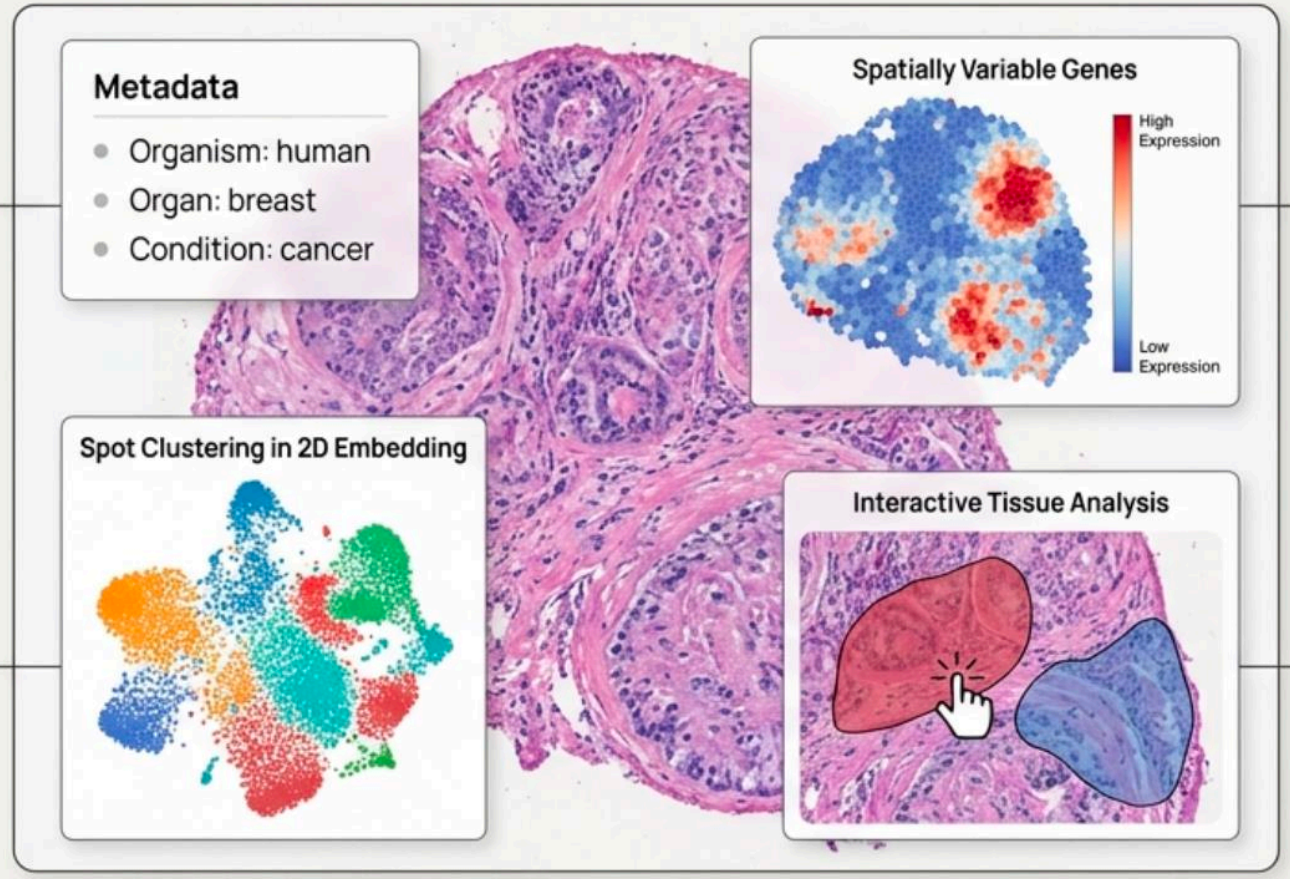


### Visualize & Analyze

Explore spatially variable genes, biological pathways, and predicted cell type compositions directly on high-resolution tissue images.

### Quality Control

Inspect and compare detailed quality metrics across thousands of samples to ensure data reliability for your analysis.

# DeepSpaceDB 2.0: A Standardized Pipeline and Viewer for 10x Xenium, Creating the Largest Public Single-Cell Spatial Atlas

## The Challenge

Publicly available 10x Xenium data is a major resource, but it's massive (>10GB per sample), highly heterogeneous, and stored in inconsistent formats.

This heterogeneity in file types, compression methods, and data structures makes large-scale analysis and direct comparison impractical.

**727 raw samples** were collected from public repositories (GEO, 10X, DBKERO) to begin the standardization process.

## The Solution

**Stage 1: Raw Data Processing**

- Ingests heterogeneous data, automatically decompressing archives, converting formats (e.g., CSV to Parquet), and repairing corrupted files.

**Stage 2: SpatialData Transformation**

- Unifies all datasets by converting them into the standardized SpatialData format, integrating expression matrices, cell boundaries, and transcript locations.

**Stage 3: Transcriptomics Analysis**

- Performs quality control, normalization, dimensionality reduction (PCA, UMAP), and spatial variability analysis (using singleCell-Haystack).

**Stage 4: Multi-Resolution Outputs**

- Generates web-optimized assets, including multi-DPI images and binned data in a compressed Zarr format for fast, interactive browser access.

**591 of 727 samples (81%) were successfully processed and standardized, forming the core of the new database.**

## The Result

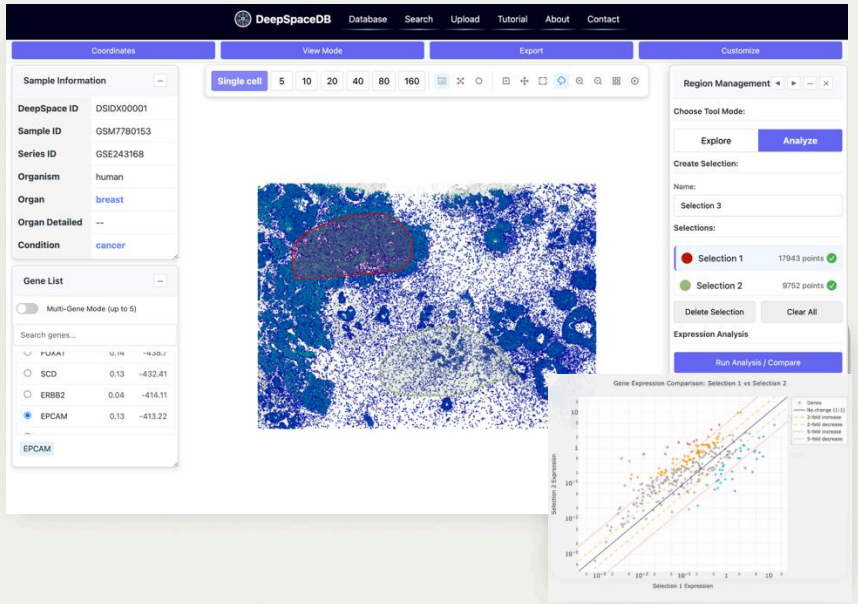


Enables fast, interactive preview of single-cell data directly in the browser, eliminating the need to download large files. Users can **visualize gene expression**, explore UMAP clusters, and compare user-selected regions of interest.

Public release planned for early 2026.